BIOCHEMISTRY
including biophysical chemistry & molecular biology

Article

pubs.acs.org/biochemistry

Conserved Walker A Cysteines 431 and 1074 in Human P-Glycoprotein Are Accessible to Thiol-Specific Agents in the Apo and ADP-Vanadate Trapped Conformations

Hong-May Sim, Jaya Bhatnagar, Eduardo E. Chufan, Khyati Kapoor, and Suresh V. Ambudkar*

Laboratory of Cell Biology, Center for Cancer Research, National Cancer Institute, National Institutes of Health, Bethesda, Maryland 20892, United States

Supporting Information

ABSTRACT: P-Glycoprotein (P-gp) is an ATP-binding cassette efflux transporter involved in the development of multidrug resistance in cancer cells. Although the mechanism of P-gp efflux has been extensively studied, aspects of its catalytic and transport cycle are still unclear. In this study, we used conserved C431 and C1074 in the Walker A motif of nucleotide-binding domains (NBDs) as reporter sites to interrogate the interaction between the two NBDs during the catalytic cycle. Disulfide cross-linking of the C431 and C1074 residues in a Cys-less background can be observed in the presence of M14M and M17M cross-linkers, which have spacer arm lengths of 20 and 25 Å, respectively. However, cross-linking with both cross-linkers was prevented in the ADP-vanadate trapped (closed) conformation. Both C431 and C1074 alone or together (double mutant) in the apo and closed conformations were found to be accessible to fluorescein 5-maleimide (FM) and methanethiosulfonate derivatives of rhodamine and verapamil. In addition, C1074 showed 1.4- and 2-fold higher degrees of FM labeling than C431 in the apo and closed conformations, respectively, demonstrating that C1074 is more accessible than C431 in both conformations. In the presence of P-gp substrates, cross-linking with M17M is still observed, suggesting that binding of substrate in the transmembrane domains does not change the accessibility of the cysteines in the NBDs. In summary, the cysteines in the Walker A motifs of NBDs of human P-gp are differentially accessible to thiol-specific agents in the apo and closed conformations.

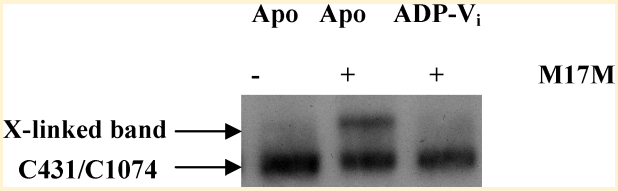

The ATP-binding cassette (ABC) superfamily constitutes one of the largest families of transport proteins.[1] Of the 48 human ABC proteins, 17 are implicated in diseases.[2] P-Glycoprotein (P-gp or ABCB1) is a clinically important ABC transporter that is involved in the development of multidrug resistance (MDR). Powered by the hydrolysis of ATP, P-gp is able to efflux various structurally dissimilar and functionally divergent chemotherapeutic drugs. Although the mechanism of efflux by P-gp has been extensively studied, there are still aspects of the catalytic and transport cycle that are not well understood.

P-gp is a single polypeptide consisting of 1280 amino acids, with two transmembrane domains (TMDs) and two nucleotide-binding domains (NBDs). While the NBDs have conserved motifs across species, the TMDs show little sequence homology. There are still unanswered questions concerning the molecular details about how ATP hydrolysis is coordinated between the two NBDs during a catalytic cycle. The current consensus is that there are three distinct conformations during one catalytic cycle of P-gp. In the absence of a transport substrate or a nucleotide, P-gp exists in the apo conformation, which is a "high-affinity inward-facing orientation" (in the shape of an inverted V). This conformation is also supported by the recent X-ray crystal structures of mouse P-gp[3] and *Caenorhabditis elegans* P-gp.[4] Before hydrolysis, there is evidence of the formation of a reaction intermediate (E·S) that can be obtained using ATP-γ-S, a nonhydrolyzable analogue of ATP.[5] In this conformation, which is temperature-dependent (occurs at 34 °C but not 4 °C), the ATP-γ-S is occluded into the P-gp NBDs. The third conformation is the ADP-vanadate (V_i) trapped posthydrolysis (E·P) conformation that assumes an outward-facing orientation (in the shape of a regular V). In the ATP-γ-S occluded and ADP-V_i trapped closed conformations, there is a reduced affinity for drug substrates.[5]

The X-ray crystal structure of P-gp in the closed conformation (in the presence of bound nucleotide) has not yet been reported. Therefore, the study of the conformational changes occurring during the catalytic cycle of P-gp is elucidated mainly by biochemical assays. Studies using disulfide cross-linking between cysteine residues in the TMDs and NBDs of P-gp in different conformations has been extensively used as a strategy to characterize these sites.[6,7] Human wild-type (WT) P-gp contains a total of seven cysteine residues, with two cysteines (C431 and C1074) in the Walker A motif of NBDs. When all the cysteines are mutated to alanines with site-directed mutagenesis, the cysteine-less (Cys-less) WT P-gp is still fully functional.[8] Therefore, cysteine residues are not essential for ATP hydrolysis or drug transport.

Received: June 17, 2013
Revised: September 13, 2013
Published: September 20, 2013

dx.doi.org/10.1021/bi4007786 | *Biochemistry* 2013, 52, 7327−7338

As C431 and C1074 line the ATP pocket of the NBDs, they are excellent sites for covalent modification by thiol-reactive probes such as fluorescein 5-maleimide (FM) and methanethiosulfonate (MTS) conjugated compounds. A more complete understanding of the accessibility of these native cysteines to thiol-specific probes would be useful in the study of conformational changes of P-gp and allow the mapping of distance changes in the NBDs during its catalytic cycle.

In this study, we determined the accessibility of conserved C431 and C1074 by disulfide cross-linking and changes in fluorescence labeling, using homobifunctional cross-linkers of various spacer arm lengths and FM, respectively. We also investigated the accessibility of these cysteines in the presence of the transport substrate, cyclosporine A (CsA). Here, we report the distance between the two NBDs of human P-gp to be 20−25 Å as the C431−C1074 distance, which is shorter than the reported distance in the X-ray crystal structure of mouse P-gp (36 Å) and *C. elegans* P-gp (54 Å). C431 and C1074 are accessible to the thiol-reactive compounds in both the apo (open) and ADP-V_i trapped (closed) conformations, with C1074 being more accessible to FM than C431. Accessibility of both the cysteines in the NBDs is not affected by the binding of the transport substrate (CsA) in the TMDs. This accessibility in both conformations of P-gp can be due to a change in the orientation of the cysteines from inward-facing to outward-facing within the ATP pocket. Thus, our results demonstrate that the cysteines in the Walker A motifs in NBDs of human P-gp are differentially accessible in the apo and closed conformations.

EXPERIMENTAL PROCEDURES

Chemicals. Homobifunctional cross-linkers M8M (3,6-dioxaoctane-1,8-diyl bismethanethiosulfonate), M14M (3,6,9,12-tetraoxatetradecane-1,14-diyl bismethanethiosulfonate), M17M (3,6,9,12,15-pentaoxaheptadecane-1,17-diyl bismethanethiosulfonate), MTS-rhodamine, and MTS-verapamil were obtained from Toronto Research Chemicals, Inc. (Downsview, ON). Cyclosporine A was purchased from Calbiochem (San Diego, CA). Fluorescein 5-maleimide (FM) was obtained from Invitrogen (San Diego, CA). P-gp-specific monoclonal antibody C-219 was obtained from Fujirebio Diagnostics Inc. (Malvern, PA). All other chemicals were obtained from Sigma Chemical Co. (St. Louis, MO).

Construction of Mutants. Histidine-tagged Cys-less wild-type (WT) P-gp was constructed by replacing the seven endogenous cysteines at positions 137, 431, 717, 956, 1074, 1125, and 1227 with alanines. Cysteine residues were reintroduced at positions 431 and 1074 individually or together into the NBDs of a histidine-tagged Cys-less P-gp cDNA as described previously.[9] In addition, N611 and T1256 were replaced individually or together with cysteine residues in a Cys-less background.

Preparation of Crude Membranes from High-Five Insect Cells Infected with Recombinant Baculovirus Carrying the Cys-less WT or Mutant Human MDR1 Gene. High-Five insect cells (Invitrogen, Carlsbad, CA) were infected with the baculovirus carrying the human MDR1 cDNA (Cys-less WT, C431, C1074, C431/C1074, N611C, T1256C, and N611C/T1256C) with a six-histidine tag at the C-terminal end as described previously.[10] Crude membranes were prepared and stored at −80 °C, as described previously.[11]

Cell Lines. HeLa cells were cultured in DMEM supplemented with 10% FBS, 1% glutamine, and 1% penicillin and maintained as described previously.[12]

Transduction of HeLa Cells with Bac-Mam Baculovirus. The BacMam-Pgp virus carrying the human MDR1 cDNA (Cys-less WT, C431, C1074, C431/C1074, N611C, T1256C, and N611C/T1256C) was added to HeLa cells (2.5 million) at a titer of 50−60 viral particles per cell in 3 mL of DMEM and was incubated for 1 h at 37 °C. Up to 20 mL of DMEM was added, and the cells were further incubated for 3−4 h. A total of 10 mM butyric acid was then added, and the cells were incubated for an additional 20 h at 37 °C. After 24 h, the cells were trypsinized, washed, counted, and analyzed by flow cytometry for cell surface expression and function. For cell surface detection of P-gp, human P-gp-specific monoclonal antibody MRK-16 was used and the fluorescence of FITC was measured on a FACSort flow cytometer equipped with a 488 nm argon laser and 530 nm bandpass filter. To assess the transport function, rhodamine 123 (1.3 μM), NBD-cyclosporin A (0.5 μM), daunorubicin (0.5 μM), and calcein-AM (0.5 μM) were used, as described previously.[12]

Vanadate-Sensitive ATPase Assay. The ATPase activity of P-gp in insect cell crude membranes was measured by the end-point inorganic phosphate (P_i) assay as previously described.[13] P-gp specific activity was recorded as the V_i-sensitive ATPase activity. Crude membranes (10−20 μg of protein/100 μL) from High-Five insect cells expressing the Cys-less WT or cysteine mutations of P-gp were incubated under different conditions with varying concentrations of compounds that were being investigated (FM, MTS-verapamil, and MTS-rhodamine) in the presence and absence of sodium orthovanadate (0.3 mM) in ATPase assay buffer [100 mM MES-Tris (pH 6.8), 100 mM KCl, 10 mM NaN_3, 2 mM EGTA, 2 mM ouabain, 20 mM $MgCl_2$, and H_2O]. The reaction was initiated by the addition of 5 mM ATP and the mixture incubated for 20 min at 37 °C. A sodium dodecyl sulfate (SDS) solution (0.1 mL of 5% SDS) was added to terminate the reaction, and the amount of P_i released was quantified with a colorimetric reaction, as described previously.[13]

Disulfide Cross-Linking with Homobifunctional Methanethiolsulfonate (MTS) Cross-Linkers and MTS Reagents. Membranes prepared from High-Five insect cells {50 μg of protein in 50 μL of buffer [10 mM Tris-HCl and 150 mM NaCl (pH 7.5)]} expressing C431 and/or C1074 as well as N611C and/or T1256C mutant P-gps in the absence of added drug substrate or ATP (apo conformation) were treated with the desired homobifunctional disulfide cross-linker (M8M, M14M, or M17M) at 200 μM for 15 min at 4 °C. To generate the ADP-V_i (closed) conformation, the membranes were first treated with 0.3 mM sodium orthovanadate, 10 mM $MgCl_2$, and 5 mM ATP at 37 °C for 20 min, and the samples were chilled at 4 °C for 5 min and then subsequently treated with the desired homobifunctional disulfide cross-linker (M8M, M14M, or M17M) at 200 μM for 15 min at 4 °C. The reactions were stopped by the addition of 5× SDS−polyacrylamide gel electrophoresis (SDS−PAGE) sample buffer without a reducing agent, β-mercaptoethanol (β-ME). The samples were subjected to SDS−PAGE [7% Tris-acetate gel (Invitrogen)] at a constant voltage of 150 V for 2 h, and immunoblot analysis was performed with P-gp-specific mouse monoclonal antibody C219 and enhanced chemiluminescence (ECL, GE healthcare) as per the manufacturer's protocol. For cross-linking with MTS reagents (MTS-verapamil and MTS-

rhodamine), High-Five insect cell membranes expressing Cys-less WT, C431, C1074, or C431/C1074 (20 μg of protein in 95 μL of ATPase assay buffer) in the apo conformation were treated with MTS-verapamil or MTS-rhodamine at 10 μM for 20 min at 4 °C. After the cross-linking reaction, 5 mM ATP (5 μL, 100 mM stock) was added to the reaction mixture and the ATPase activity was evaluated as described previously.

Labeling with Fluorescein 5-Maleimide and Fluorescence Spectroscopy. Fluorescein 5-maleimide was used to label the P-gp single- and double-cysteine mutants in both the apo and closed conformations. Briefly, 100 μg of protein/50 μL of crude membranes from the High-Five insect cells expressing Cys-less WT and C431/C1074 and N611C/T1256C (single- or double-cysteine mutants) in the apo form, Mg^{2+}-ATP, and Mg^{2+}-ATP with 0.3 mM V_i to generate ADP-V_i (closed conformation) was incubated with 100 μM FM in 2% DMSO for 5 min at 37 °C in the dark. (The level of P-gp protein in insect cell crude membranes is ∼2%. For labeling with FM, 0.28−0.30 μM P-gp was used and there was a 330-fold molar excess of FM.) To generate the closed conformation, the crude membranes were first incubated with 0.3 mM V_i, 20 mM $MgCl_2$, and 10 or 20 mM ATP and incubated for 10 min at 37 °C. To make sure the cysteine mutants remained in the closed conformation before being cross-linked with FM, 10 μg of protein sample that was treated with ATP and V_i to generate the ADP-V_i (closed) conformation was assessed for ATPase activity. Following this, 100 μM FM was added for 5 min at 37 °C in the dark. The reaction was then quenched with 5 μL of 500 mM EDTA and 12.5 μL of 5× SDS−PAGE sample buffer. For immunoprecipitation of FM-labeled P-gp, 700 μL of RIPA buffer and 10.5 μg of antibody C219/100 μg of P-gp were added, and the reaction mixture was incubated at room temperature for 30 min in the dark while being rocked. Protein A Sepharose beads (35 μL) in RIPA buffer were added and further incubated for 2.5 h while being rocked in the dark. The beads were pelleted by centrifugation at 13000 rpm for 5 min at 4 °C. The beads were washed three times with RIPA buffer (800 μL) and twice with 800 μL of 50 mM Tris-HCl (pH 7.5) supplemented with 500 mM NaCl; 2× SDS−PAGE sample buffer (25 μL) without β-ME was added, followed by incubation at 42 °C for 30 min. A further 25 μL of deionized water was added, and the mixture was incubated at 42 °C for an additional 30 min before samples were subjected to SDS−PAGE (7% Tris-acetate gel) at a constant voltage of 150 V for 1.5 h. The gel was scanned for blue fluorescence, and the fluorescence incorporated into the P-gp band was quantified using the STORM 860 BlueFluorescence Imager system (Molecular Dynamics, Sunnyvale, CA) and ImageQuaNT. The fluorescence incorporated into Cys-less WT and C431/C1074 P-gp is quantified by ImageQuaNT and then corrected for background fluorescence in the respective lanes. The expression levels of P-gp in the cysteine mutants were determined by colloidal blue staining of the same gel that was used for fluorescence imaging and quantification. The protein levels of mutant P-gps (C431, C1074, and C431/C1074) are expressed as a ratio relative to Cys-less WT by quantifying the amount of colloidal blue-stained mutant P-gps and normalizing it to the amount of Cys-less WT. The final level of fluorescence (in arbitrary units) was calculated as (FM fluorescence incorporated into P-gp mutant − background fluorescence)/(ratio of mutant P-gp expression relative to Cys-less WT protein).

Molecular Modeling. A homology model of human P-gp in an open, inward-facing conformation was built on the basis of the X-ray structure of QZ59-*RRR*-bound mouse P-gp [Protein Data Bank (PDB) entry 3G60].[3] The model was generated using only one molecule (chain A) of the two present in the crystal asymmetric unit. The sequence alignment was done by BLAST.[14] The model was constructed by *in silico* mutation of the protein residues to the human P-gp sequence, and three residues (D87-L88-M89, absent in the mouse mdr1a-P-gp sequence) were manually modeled at extracellular loop 1 (ECL1). Finally, side-chain conformations of the new residues were visually inspected and modified when necessary. The stereochemical quality of the models was inspected by PROCHECK;[15] some fragments of the structures were submitted to geometrical regularization using Coot[16] to improve the stereochemical quality. The final structure had only two close contacts (A198 O to T202 OG1, 2.18 Å; and P66 CB to T202 OG1, 2.19 Å), and a Ramachandran plot showed 73.7% residues in most favored regions, 19.5% in additional allowed regions, 6.8% in generously allowed regions, and no residues in disallowed regions.

The homology model of human P-gp in the closed, outward-facing conformation was assembled with the NBD domains built on the basis of the Hly-B structure, as described by Ohnuma et al.,[17] and the TMD constructed by O'Mara and Tieleman, on the basis of the *Staphylococcus aureus* Sav1866 structure. The NBDs and TMDs fit together very well, and the joint areas were regularized and carefully inspected using Coot;[16] the emerging model was finally energy-minimized by CHARMm.[18]

Docking studies of FM at the NBDs of the homology model of human P-gp based on the X-ray structure of Hly-B were conducted using AutoDock Vina.[19] The receptor and ligand structures were prepared with the MGLtools software package.[20] Docking jobs were conducted in the free ATP site model, at ATP site 1 with the K433 side chain set as flexible and the search box centered at the γ-phosphate of the original ATP molecule ($x = -2.295$, $y = 5.702$, $z = -4.443$) with dimensions of 16 Å × 12 Å × 18 Å and at ATP site 2 with the K1076 side chain set as flexible and the search box centered at the γ-phosphate of the original ATP molecule ($x = 1.499$, $y = -6.416$, $z = 12.957$) with dimensions of of 20 Å × 20 Å × 18 Å. Docking jobs were also run in the model with ATP, at ATP site 1 with C431 in an outward-facing orientation using a rotamer taken from the library of Pymol and the search box centered at the sulfur atom of C431 ($x = 1.734$, $y = 10.9$, $z = -8.889$) with dimensions of 30 Å × 10 Å × 16 Å and at ATP site 2 with C1074 in an outward-facing orientation using a rotamer taken from the library of Pymol and the search box centered at the sulfur atom of C1074 ($x = 7.63$, $y = -8.705$, $z = 17.29$) with dimensions of 18 Å × 28 Å × 24 Å.

RESULTS

Homology Models of Human P-Glycoprotein. The model of full-length human P-gp in the apo form (open conformation) was built on the basis of the X-ray structure of mouse P-gp,[3] while the model of human P-gp in the nucleotide-bound form (also called the closed conformation) was built using the TMD model built by O'Mara and Tieleman[21] on the basis of the structure of Sav1866[22] and the NBD model based on the structure of Hly-B[23] (Figure 1). The Hly-B structure was chosen for these studies because it was crystallized with ATP

dx.doi.org/10.1021/bi4007786 | *Biochemistry* 2013, 52, 7327−7338

and Mg^{2+}, while the Sav1866 protein was crystallized in the presence of ADP and Na^{+}.

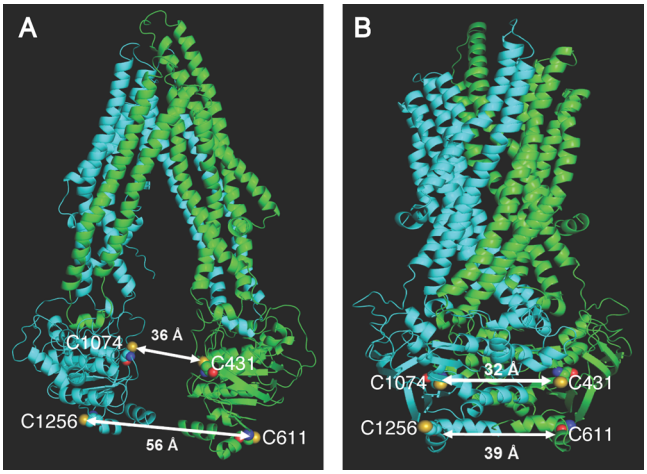

Figure 1. Homology models of human P-glycoprotein. Models of human P-gp in the apo form (open conformation) based on the X-ray structure of mouse P-gp (A) and in the nucleotide-bound form (closed conformation) based on an assembled model of Sav1866-TMD and Hly-B-NBD (B) were generated as described in Experimental Procedures. (A) Locations of cysteine mutants in NBDs in the apo conformation. The distances between cysteines 431 and 1074 and cysteines 611 and 1256 are 36 and 56 Å, respectively. (B) Locations of cysteine mutants in NBDs in the closed conformation. The distances between cysteines 431 and 1074 and cysteines 611 and 1256 in the closed conformations are 32 and 39 Å, respectively. The N-terminal and C-terminal ends of P-gp are colored green and cyan, respectively; oxygens are colored red, nitrogens blue, and sulfurs yellow.

Walker A C431 and C1074 located in NBD1 and NBD2, respectively, were selected for distance measurements using disulfide cross-linkers. This pair of cysteine residues was selected as they are native cysteines lining the ATP sites of the NBDs. The other pair of cysteine residues selected in this study were N611C and T1256C, and they are located on the surface of the NBDs, away from the ATP-binding sites. From these homology models, the predicted distances between C431 and C1074 in the apo and closed conformations are 36 and 32 Å, respectively. The predicted distances between N611C and T1256C in the apo and closed conformations are 56 and 39 Å, respectively (Figure 1).

Cell Surface Expression and Transport of Fluorescent Substrates by C431/C1074 and N611C/T1256C Mutant P-gps in HeLa Cells. The cell surface expression of C431/C1074, measured by MRK-16 staining, was similar to that of Cys-less WT (100% compared to that of Cys-less WT), while the cell surface expression of N611C/T1256C was 50% lower than that of Cys-less WT (Figure 2A,B). Despite the somewhat lower level of cell surface expression of N611C/T1256C, both pairs of NBD cysteine mutants exhibited normal transport function (90−100%) with P-gp substrates, rhodamine 123, NBD-cyclosporine A, daunorubicin, and calcein-AM. Panels C and D of Figure 2 show typical histograms for transport function with rhodamine 123 as a substrate for these two double-cysteine mutants. The transport function of mutant P-gps tested with four commonly used fluorescent substrates is summarized in Table S1 of the Supporting Information.

Disulfide Cross-Linking with Homobifunctional Cross-Linkers of Cys-less WT and C431/C1074 and N611C/T1256C Mutant P-gps in Apo and Closed Conformations. Crude membranes prepared from High-Five insect cells expressing C431/C1074 or N611C/T1256C in apo and closed conformations were treated with M8M, M14M, and M17M (with spacer arm lengths of 13, 20, and 25 Å, respectively). The results are shown in Figure 3. Figure 3A shows the positions of the cross-linked (X-linked) (upper band) and un-cross-linked (lower band) P-gp obtained in the apo state. Cross-linking with M14M and M17M occurs in the apo conformation of P-gp (Figure 3A), but not in the closed conformation (Figure 3B). With a shorter cross-linker (M8M), cross-linking is absent in both conformations (Figure 3A). In the presence of 5 mM DTT (a reducing agent), there is inhibition of cross-linking, indicating that cross-linking is mediated by disulfide bond formation (Figure 3C). We also found that the mobility of Cys-less WT and C431/C1047 mutant P-gp on the gel in the apo and ADP-V_i closed conformation in the absence of cross-linkers was not altered (data not shown). In Cys-less WT, as expected, there was no cross-linking in either tested conformation (Figure 3D). In addition, treatment of the single-cysteine mutants C431 and C1074 with M17M did not result in cross-linking (data given in Figure S1 of the Supporting Information). As a comparison, N611C/T1256C was treated with M17M. As shown in Figure S2 of the Supporting Information, there was no cross-linking. This result is consistent with the greater separation of N611C and T1256C with a predicted distance of 56 Å in the apo conformation compared to C431 and C1074 with a predicted distance of 36 Å from the homology model of human P-gp (Figure 1). The data in Figure 3B demonstrate that C431 and C1074 in the apo conformation can come much closer (20−25 Å) than the distance predicted by homology models or the distance observed in the crystal structure of mouse P-gp.[3]

FM Labeling of Cys-less WT, C431, C1074, C431/C1074, N611C, T1256C, and N611C/T1256C in Apo and Closed Conformations. Crude membranes prepared from High-Five insect cells expressing single-cysteine (C431, C1074, N611, and T1256) and double-cysteine (C431/C1074 and N611C/T1256C) mutants in both the apo and closed conformations were labeled with FM. A vanadate-sensitive ATPase assay confirmed that C431/C1074 remained in the closed conformation prior to cross-linking with FM (Figure S3 of the Supporting Information), as its ATPase activity was inhibited >90% in the presence of V_i. As seen from the fluorogram in Figure 4A, quantification of the FM-labeled P-gp showed that C431 is less labeled than C1074 in both the apo and closed conformations. With C431 and C1074, there is a similar extent of FM labeling in both conformations. The extent of labeling in the double-cysteine mutant is ~2 times that of the individual single-cysteine mutants in both conformations, with fluorescence intensity contributed by FM. There were no significant differences observed between the two conformations with C431/C1074. These results suggest that there are differential accessibilities of C431 and C1074 in both conformations.

The quantification of the FM-labeled P-gp after normalization with P-gp expression for each mutant (Figure 4B) showed that single-cysteine mutants N611C and T1256C in both conformations are labeled with FM to similar extents. Similar to C431/C1074, the extent of FM labeling in the double-cysteine mutants, after normalization of protein expression, is ~2 times that seen with the individual single-cysteine mutants in both conformations. With N611C/

dx.doi.org/10.1021/bi4007786 | *Biochemistry* 2013, 52, 7327−7338

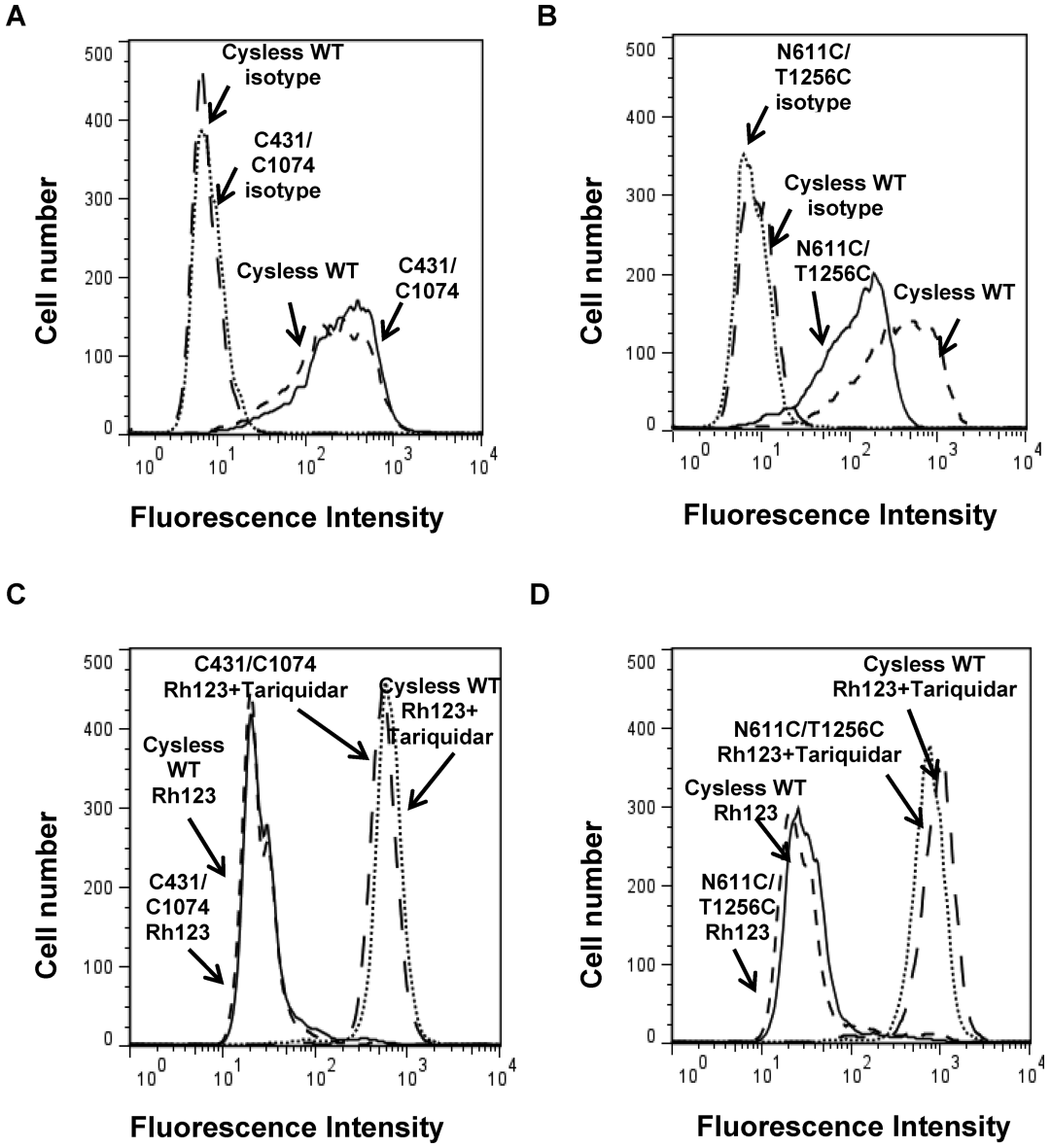

Figure 2. Cell surface expression and transport function of C431/C1074 and N611C/T1256C mutant P-gps expressed in HeLa cells. (A) C431/C1074 and (B) N611C/T1256C mutant P-gps have cell surface expression similar to that of Cys-less WT. HeLa cells transduced with mutant P-gp BacMam virus were evaluated for their cell surface expression by incubation with the MRK-16 antibody for 1 h, followed by the FITC-labeled anti-mouse secondary antibody for 30 min. (C) C431/C1074 and (D) N611C/T1256C mutant P-gps have normal transport function similar to that of Cys-less WT. The HeLa cells were incubated in the presence and absence of 1 μM tariquidar and 0.5 mg/mL rhodamine 123 (Rh123) for 45 min. Cells were washed and analyzed by flow cytometry. The histograms represent fluorescence intensity (x-axis) plotted as a function of cell number (y-axis) and are representative of three independent experiments. The figure represents a typical histogram for cell surface expression and transport function with the substrate rhodamine 123 (Rh123), for C431/C1074 (A and C) and N611C/T1256C (B and D).

T1256C, no significant difference was observed between the apo and closed conformations, suggesting the accessibilities of these single-cysteine mutants to FM are similar in both conformations. In Cys-less WT, as expected, there was only background labeling with FM (<20%) as seen in both panels A and B of Figure 4.

When the NBDs are supersaturated with 20 mM ATP (with 20 mM $MgCl_2$) (closed conformation) (Figure 4C) prior to labeling with FM, labeling was observed to an extent similar to that seen for the apo conformation. This result shows that the C431 and C1074 residues are oriented in a direction that is still accessible for FM labeling when the ATP is bound to both NBDs.

Inhibition of ATPase Activity with FM, MTS-Verapamil, and MTS-Rhodamine. FM is a thiol-reactive probe that reacts with cysteines, and verapamil and rhodamine are substrates of P-gp. We wanted to test whether like FM, MTS-verapamil and MTS-rhodamine can also label the cysteine residues in the NBDs. For this, V_i-sensitive ATP hydrolysis of these cysteine mutants after cross-linking with MTS-verapamil and MTS-rhodamine was assessed. With Cys-less WT, there is minimal inhibition of ATP hydrolysis (<20%) by FM, indicating FM had no effect on this activity (Figure 5). With C431 and C1074 single- and double-cysteine (C431/C1074) mutants that line the ATP pocket, the ATP hydrolysis activity was drastically inhibited with IC_{50} values of 1.1 ± 0.2 μM for C431, 0.7 ± 0.1 μM for C1074, and 0.63 μM for C431/C1074

dx.doi.org/10.1021/bi4007786 | Biochemistry 2013, 52, 7327−7338

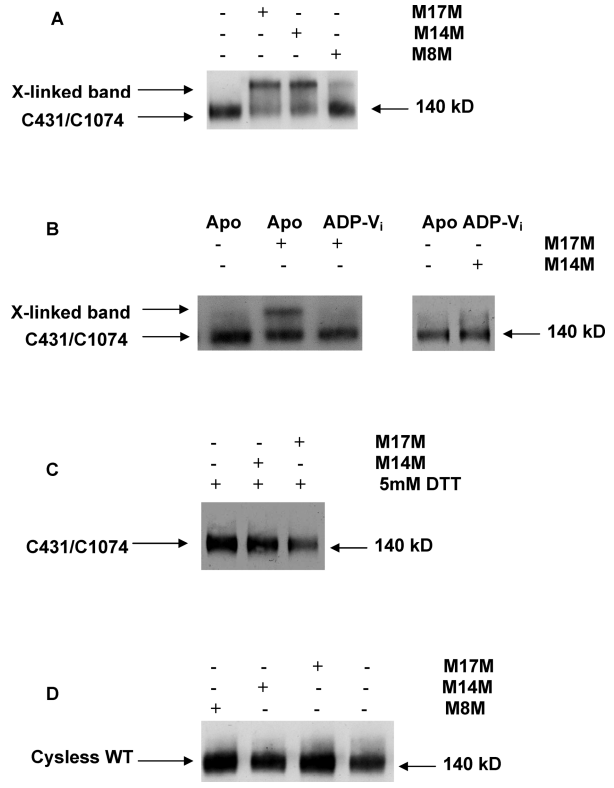

Figure 3. Disulfide cross-linking of C431/C1074 with homobifunctional cross-linkers M8M, M14M, and M17M in the apo and ADP-V_i trapped states and in the presence and absence of 5 mM DTT. (A) Disulfide cross-linking of C431/C1074 with M8M, M14M, and M17M in the apo conformation. Panel A shows the positions of the cross-linked (X-linked) and the lower un-cross-linked P-gp with different cross-linkers. Membranes prepared from High-Five insect cells expressing C431/C1074 (50 μg) were treated with 200 μM disulfide cross-linkers M8M, M14M, and M17M for 15 min at 4 °C. The reactions were stopped by the addition of SDS sample buffer containing no reducing agent (β-ME), and samples were subjected to immunoblot analysis via SDS–PAGE (7% Tris-acetate gel) as described in Experimental Procedures. (B) Disulfide cross-linking of C431/C1074 with M14M and M17M in the apo and ADP-V_i trapped states. Panel B shows the positions of the cross-linked (X-linked) and un-cross-linked P-gp with M14M and M17M in different conformational states. To generate the ADP-V_i trapped closed conformation, C431/C1074 (50 μg) was incubated with 0.3 mM V_i, 10 mM $MgCl_2$, and 5 mM ATP and the sample was incubated for 10 min at 37 °C, as described in Experimental Procedures. Subsequently, the sample was chilled to 4 °C for 5 min, and the cross-linkers (200 μM) were added and incubated for 20 min at 4 °C. (C) Disulfide cross-linking of C431/C1074 with M14M and M17M in the presence and absence of 5 mM DTT. Panel C shows the inhibition of cross-linking in the presence of 5 mM DTT. (D) Disulfide cross-linking of Cys-less WT with cross-linkers M8M, M14M, and M17M in the apo conformation. Panel D shows the absence of cross-linking of Cys-less WT with the various cross-linkers.

(Figure 5A). These results indicate that the observed effect of FM was due to its interaction with these cysteine residues. The lower IC_{50} values (concentration to inhibit 50% ATPase activity in the presence of a thiol-reactive probe) for C1074 compared to those for C431 in all cases indicated that C1074 was more accessible to FM for modification than C431, consistent with labeling of these residues with FM (Figure 4).

When conjugated with a MTS moiety, MTS-verapamil and MTS-rhodamine are reactive toward the cysteine residues. The specificity of the Walker A cysteines toward thiol-reactive probes was also confirmed with MTS-verapamil and MTS-rhodamine, which have different bulk and size compared to FM (Figures S4 and S5 of the Supporting Information). With MTS-verapamil, a concentration-dependent biphasic effect on the ATPase activity of Cys-less WT and the single and double C431/C1074 mutants was observed. At a low concentration of less than 1–2 μM, MTS-verapamil marginally stimulated ATP hydrolysis of Cys-less WT and the single and double C431/C1074 mutants (100–120% ATPase activity). This stimulatory effect might possibly be due to noncovalent interaction of MTS-verapamil with P-gp, with the dominant effect of the verapamil moiety functioning as a substrate versus the MTS moiety for covalent interaction with the cysteine residue(s). At concentrations of >2 μM, there was inhibition of ATPase activity seen with all the cysteine mutants because of the covalent modification of the thiol group by MTS. There was no inhibition of ATPase activity observed for Cys-less WT, as expected.

With 10 μM MTS-verapamil and MTS-rhodamine, there was inhibition of P-gp ATPase activity for single and double C431/C1074 mutants [ATPase activity is reduced to 20–40% compared to a basal activity of 100% for MTS-verapamil (Figure S4 of the Supporting Information), and ATPase activity is 50–80% compared to basal activity for MTS-rhodamine (Figure S5 of the Supporting Information)].

With N611C or T1256C, the formation of a cross-linked FM-labeled product did not drastically inhibit ATPase hydrolysis and the IC_{50} values of FM could not be determined for these mutants. The maximal levels of ATPase inhibition by FM in N611C, T1256C, and N611C/T1256C were 39, 11, and 56%, respectively (Figure S6 of the Supporting Information).

Reversibility of Covalent Modification of C431, C1074, or C431/C1074 Mutant P-gps by FM, MTS-Verapamil, and MTS-Rhodamine. To test the reversibility of the disulfide-mediated covalent modification of the cysteine residues in the NBD mutants, 4 mM DTT was added to C431 and C1074 and single- and double-cysteine C431/C1074 mutants after cross-linking with 10 μM MTS-verapamil and MTS-rhodamine; 10 μM MTS-verapamil or MTS-rhodamine was chosen, as there is ~70% inhibition of ATPase activity in the NBD mutants. As shown in Figure S5 of the Supporting Information, the ATPase activity of MTS-verapamil cross-linked NBD mutants was stimulated >3-fold compared to the basal activity after the addition of 4 mM DTT. With MTS-rhodamine in the presence of 4 mM DTT, the ATPase activity was stimulated to a level higher than basal activity but the stimulation was not as great as in the case with MTS-verapamil. In both cases, stimulation of ATPase activity indicated the reversibility of ATPase activity by the breakage of the disulfide bond with 4 mM DTT. For FM-cross-linked C431/C1074 (Figure 5C), the presence of 4 mM DTT did not restore the ATPase hydrolysis of P-gp in either of the conformations, confirming the covalent thioether-mediated modification of the cysteine residues by the maleimide moiety.

Pretreatment with ATP Protects C431, C1074, or C431/C1074 Mutant P-gps from Cross-Linking with MTS Compounds and FM. As both C431 and C1074 line the ATP pocket, we hypothesized that protection of the pocket by preincubation with 5 mM ATP and 20 mM $MgCl_2$ would prevent FM from occupying the pocket and hence restore ATP hydrolysis. As expected, the ATPase activities of C431, C1074, and C431/C1074 were all protected from inactivation by FM

dx.doi.org/10.1021/bi4007786 | *Biochemistry* 2013, 52, 7327–7338

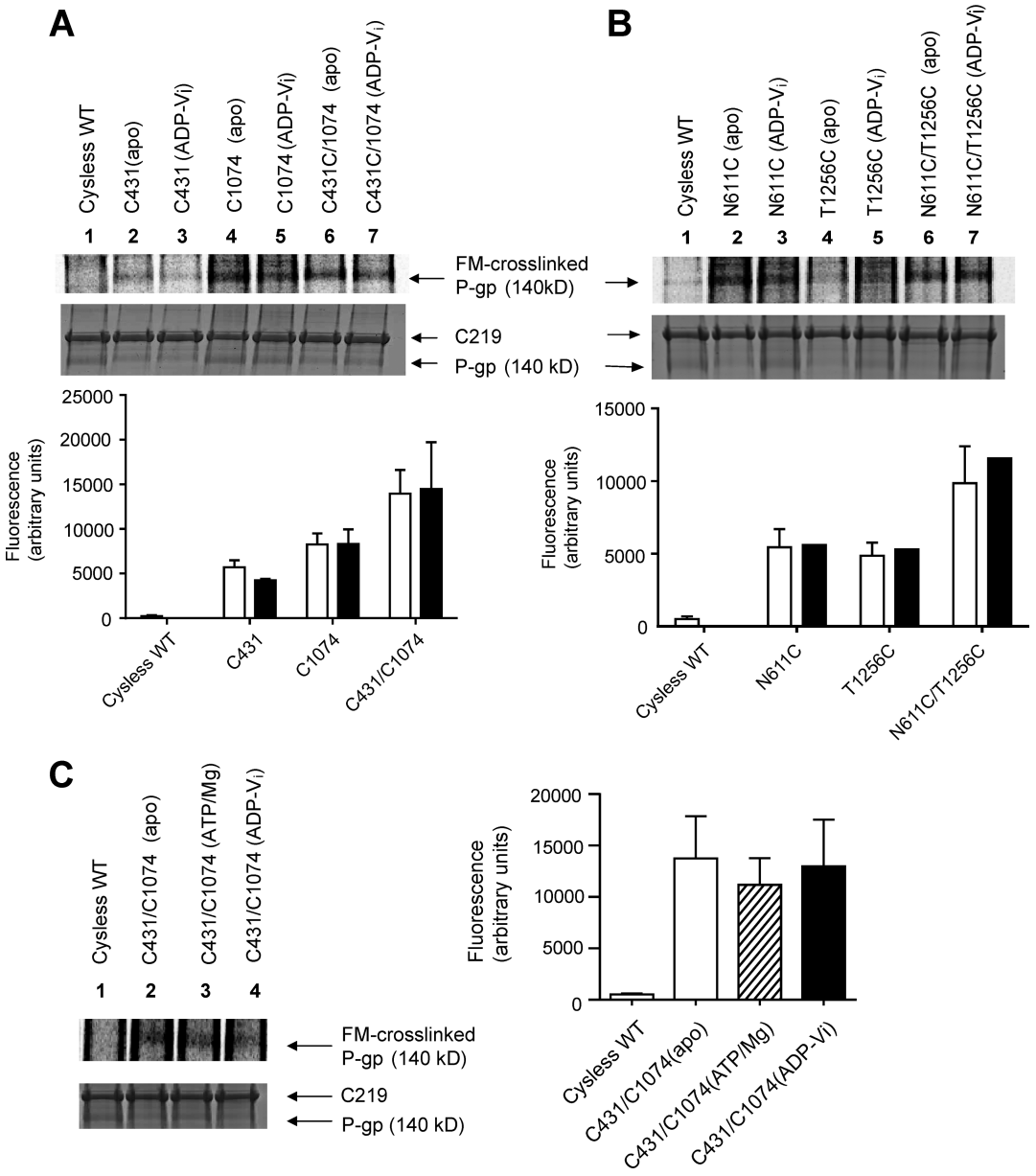

Figure 4. Labeling of Cys-less WT and single- and double-cysteine mutant P-gps with fluorescein maleimide. (A) Fluorogram (top) and quantification of fluorescence labeling using ImageQuaNT of Cys-less WT, C431, C1074, and C431/C1074 cysteine mutants in the apo and ADP-V_i trapped conformations. The DTT-free crude membranes of High-Five insect cells expressing Cys-less WT, C431, C1074, or C431/C1074 were cross-linked with 100 μM fluorescein maleimide for 5 min at 37 °C. To generate the ADP-V_i trapped closed conformation, single- and double-cysteine mutant P-gps were first incubated with 0.3 mM V_i, 20 mM $MgCl_2$, and 10 mM ATP, and the samples were incubated for 10 min at 37 °C prior to cross-linking with FM, as described in Experimental Procedures. The reactions were stopped by the addition of NEM (5 mM) and EDTA (50 mM) and followed by immunoprecipitation of P-gp with C219, as described in Experimental Procedures. (B) Fluorogram (top) and quantification of fluorescence labeling using ImageQuaNT of Cys-less WT, N611C, T1256C, and N611C/T1256C cysteine mutants in the apo and ADP-V_i trapped conformations. The DTT-free crude membranes of High-Five insect cells expressing N611C, T1256C, and N611C/T1256C in both the apo and ADP-V_i trapped conformations were cross-linked with 100 μM FM as described for panel A. The reactions were stopped by the addition of NEM (5 mM) and EDTA (50 mM) and followed by immunoprecipitation of P-gp with C219 as described in Experimental Procedures. The same gel was stained with colloidal blue dye for detection of P-gp expression (bottom), as described in Experimental Procedures. The average values from two independent experiments for the ADP-V_i trapped condition are shown. (C) Fluorogram and quantification of fluorescence labeling using ImageQuaNT of Cys-less WT and C431/C1074 mutants in the apo conformation, in the presence of saturating ATP (20 mM) and $MgCl_2$ (20 mM) and ADP-V_i trapped conformations. The DTT-free Cys-less WT and C431/C1074 in the apo state, in the presence of saturating ATP (20 mM) and $MgCl_2$ (20 mM), and in the ADP-V_i trapped conformations were cross-linked with 100 μM FM. In this experiment, 0.3 mM V_i, 20 mM $MgCl_2$, and 20 mM ATP were added to generate the ADP-V_i conformation, and the samples were incubated for 10 min at 37 °C prior to treatment with FM, as described in Experimental Procedures. The gels in panels A–C were stained with colloidal blue dye for detection of P-gp expression as described in Experimental Procedures, fixed, and air-dried in DryEase mini cellophane (Novex). The scans of stained air-dried gels are shown under the respective fluorogram in panels A–C. The quantified data are shown in the histogram and represent the average of at least two experiments. Data with error bars denote the standard deviation (n = 3).

dx.doi.org/10.1021/bi4007786 | *Biochemistry* 2013, 52, 7327–7338

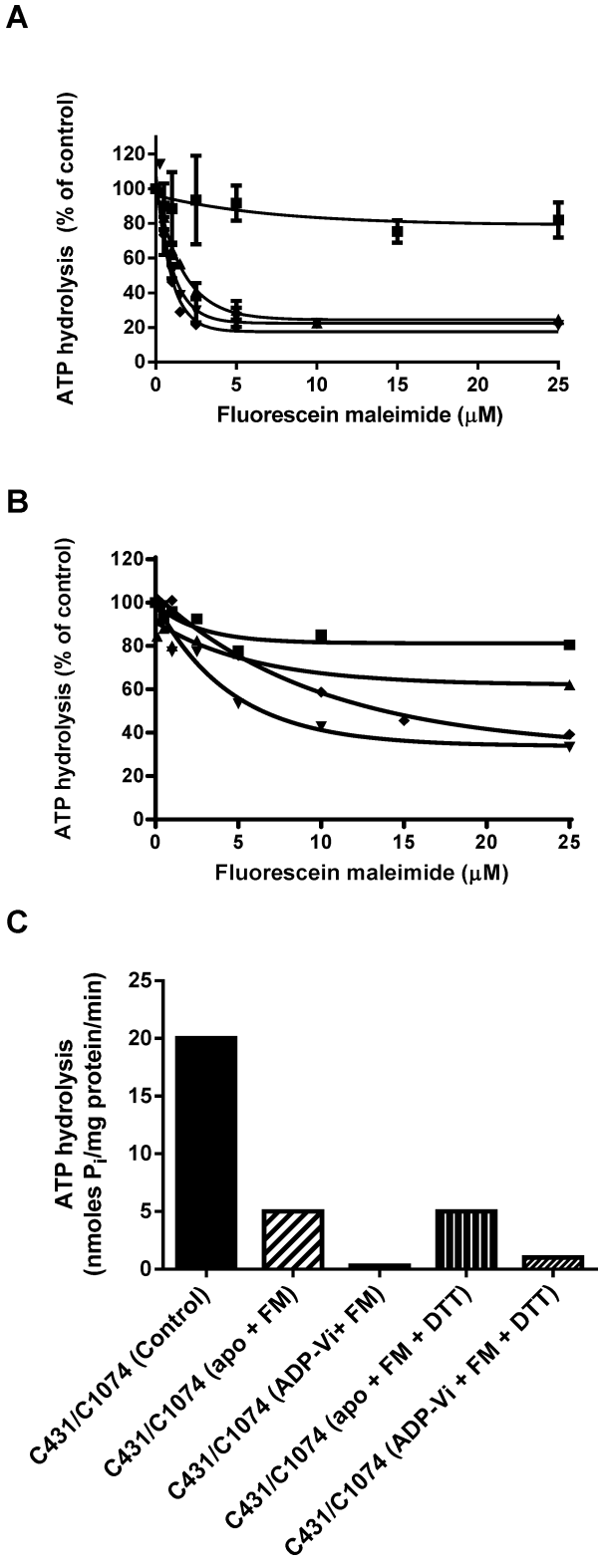

Figure 5. Effect of fluorescein maleimide on ATP hydrolysis by Cys-less WT, single-mutant C431 and C1074, and double-mutant C431/C1074 P-gps. (A) Inhibition of P-gp ATPase activity by FM in Cys-less WT (■), C431 (▲), C1074 (▼), and C431/C1074 (◆). Vanadate-sensitive P-gp-mediated ATPase hydrolysis was assessed as described in Experimental Procedures in the presence of increasing concentrations of FM (0–25 μM). FM was incubated with the respective cysteine mutants (10–20 μg of protein/100 μL) for 5 min at room temperature prior to the addition of 5 mM ATP. The IC_{50} (FM) for inhibition of P-gp-mediated ATP hydrolysis in Cys-less WT cannot be determined, as FM does not interact with Cys-less P-gp. The IC_{50} (FM) values for C431, C1074, and C431/C1074 are 1.1 ± 0.15, 0.70 ± 0.1, and 0.63 μM, respectively. (B) Inhibition of P-gp ATPase activity by FM after preincubation with 5 mM ATP in C431, C1074, and C431/C1074. ATP (5 mM) and $MgCl_2$ (20 mM) were added to the reaction mixture on ice for 5 min with the respective cysteine mutants (10–20 μg of protein/100 μL) prior to the addition of various concentrations of FM. The IC_{50} (FM) for inhibition of P-gp-mediated ATP hydrolysis in Cys-less WT, C431, C1074, and C431/C1074 cannot be determined when 5 mM ATP is added prior to FM due to partial inhibition. (C) Irreversibility of ATPase activity after addition of 4 mM DTT. In this experiment, 5 μg of C431/C1074 cross-linked with 100 μM FM in both the apo and closed conformations was evaluated for ATPase activity with and without 4 mM DTT. Data represent the mean values (error bars show means ± the standard deviation for $n = 3$). In panels A and B, IC_{50} curves were generated by nonlinear regression (one-phase decay) using GraphPad Prism 5.

by pretreatment with 5 mM ATP and 20 mM $MgCl_2$ prior to the addition of FM. The IC_{50} values of FM in these single- and double-cysteine mutants could not be determined under these conditions, as the maximal levels of inhibition of ATP hydrolysis of 38, 66, and 68% was observed for C431, C1074, and C431/C1074, respectively (Figure 5B).

For N611C and T1256C mutants, as expected, there was no change in the ATP hydrolysis profile with or without 5 mM ATP. In both cases, the IC_{50} values of FM in these single- and double-cysteine mutants could not be determined (Figure S6 of the Supporting Information). In the presence of 5 mM ATP, the maximal levels of inhibition of ATPase hydrolysis in these cysteine mutants were 26, 27, and 51% in N611C, T1256C, and N611C/T1256C, respectively. These results were expected, because cysteine mutants N611C and T1256C are on the surface of the NBDs and are fully accessible to covalent modification by FM even in the presence of ATP.

Preincubation with 10 mM ATP protects C431 and C1074 single- and double-cysteine mutants from reaction with MTS-verapamil or MTS-rhodamine (10 μM) by saturating the ATP pocket. As shown in Figure S5 of the Supporting Information, the ATPase activity was retained at 50–90% of basal activity as compared to the greater inhibition when the order of addition was reversed (MTS compounds followed by ATP). The ATPase activity of C431 is restored to a greater level than that achieved with C1074. This result confirms the greater accessibility of C1074 than of C431 for covalent modification.

Pretreatment with Drug Substrates Does Not Inhibit Cross-Linking of C431/C1074 Mutant P-gp with FM and M17M. Disulfide cross-linking is seen in C431/C1074 with the M17M cross-linker in the apo conformation. To determine whether binding of transport substrates in the drug-binding pocket in the TMDs[7,24] has any effect on the accessibility of C431 and C1074 for cross-linking with thiol-reactive agents, C431 and C1074 were first treated with substrates CsA (50 μM), QZ 59 SSS (20 μM), and actinomycin D (200 μM) and then with M17M. These results are given in Figure S7 of the Supporting Information, and the immunoblot in this figure demonstrates that pretreatment with a transport substrate or modulator that binds in the TMDs has no effect on the conformation of NBDs for cross-linking in the absence of ATP. We also determined whether the accessibility of the cysteines to FM is changed in the presence of 50 μM CsA prior to the

dx.doi.org/10.1021/bi4007786 | Biochemistry 2013, 52, 7327–7338

addition of various concentrations of FM. The IC_{50} value of FM for inhibition of ATP hydrolysis by the C431/C1074 double mutant was similar in the absence of CsA (2 μM) and in the presence of CsA (1.4 μM) (Figure 6).

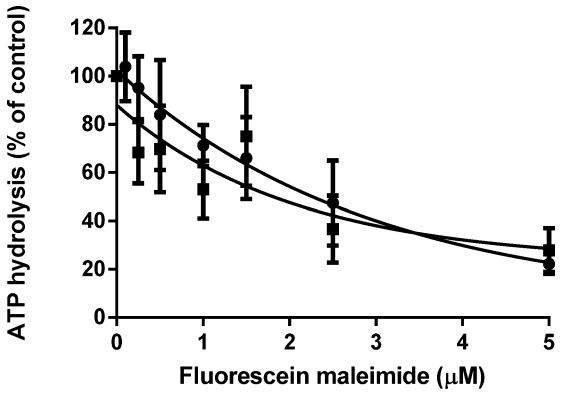

Figure 6. Effect of cyclosporine A on C431/C1074 double mutant P-gp-mediated ATP hydrolysis in the presence of increasing concentrations of FM. Vanadate-sensitive ATPase hydrolysis by the double-cysteine mutant was measured as described in Experimental Procedures in the presence of increasing concentrations of FM (0–5 μM) after preincubation without substrate (●) and with 50 μM CsA (■). In this experiment, 50 μM CsA was incubated with C431/C1074 (20 μg of protein/100 μL) for 5 min at room temperature prior to the addition of 5 mM ATP. The IC_{50} (FM) values for inhibition of P-gp-mediated ATP hydrolysis in the absence and presence of CsA are 2.0 ± 0.2 and 1.4 μM, respectively. Data represent the mean values (error bars show the standard deviation for n = 3). IC_{50} curves were generated by nonlinear regression (one-phase decay) using GraphPad Prism 5.

Docking Studies of FM at the ATP Sites. Using the homology model of human P-gp ATP sites based on Hly-B, docking studies of FM were conducted at the ATP sites with the aim of correlating biochemical data with molecular structural information. It is known that the maleimide group is reactive toward cysteine residues. Further, the X-ray structure of the FM-labeled class A β-lactamase PenP deposited in PDB (entry 3M2J) shows the FM molecule covalently bound to a cysteine through one of the carbon atoms of the maleimide ring. Therefore, docking studies were designed to find conformations of FM, at the ATP sites and outside ATP sites, with the reactive carbon of the maleimide ring pointing toward the Walker A cysteines. Several runs using different search boxes were conducted. Walker A lysines (K433 and K1076) that prevent modeling the FM molecule closer to the C431 and C1074 were set as flexible residues when FM was docked within the ATP sites. The poses that have the maleimide ring pointing toward the Walker A cysteines with the shortest S(Cys)–C(maleimide) distances were selected (black dashed line in each panel in Figure 7).

In ATP site 1, an FM molecule is found at the same position and orientation as ATP, sandwiched between the Walker A motif of NBD1 and the signature motif of NBD2. It is interesting to note that one of the carbonyl groups of the reactive maleimide ring forms hydrogen bonds with the side chain of neighboring residues, suggesting that these residues (E556 and S434) could play a relevant role in orienting the reactive carbons toward the C431 residue. In ATP site 2, the docked FM molecule is found at a position different from that of ATP, although with the reactive C (maleimide) pointing toward C1074 (Figure 7 A and C). It is difficult to know which residue(s) or loops are responsible for preventing the FM molecule from docking at the same position as ATP.

Docking of FM at the ATP sites with bound ATP was also conducted (Figure 7 B and D). In the vicinity of ATP site 1, the FM molecule fits very well in a site defined by the loops of residues 407–409 and 602–604 and the α-helix of residues 1154–1161. FM was also docked in the equivalent site in the vicinity of ATP site 2; it is surrounded by the α-helix and loops equivalent to those that defined the site in the vicinity of ATP site 1 (residues 509–516, 1247–1249, and 1050–1052, respectively). At both sites, the carbonyl groups of the maleimide ring form hydrogen bonds with neighboring residues (D603 and Q1180 at site 1 and N1248 and Q535 at site 2).

■ DISCUSSION

On the basis of the X-ray crystal structures of mouse P-gp, Sav1866, and Hly-B, homology models of human P-gp in both apo and closed conformations were built (Figure 1). Cysteines 431 and 1074 in the Walker A motifs of P-gp are conserved across many species. Hence, these native cysteines are excellent reporter sites for studying the interaction between the two NBDs of P-gp. In this study, we selected N611C/T1256C as the other pair of double-cysteine mutant P-gp (on the surface of the NBDs) located away from the ATP-binding sites. The distances in the apo and closed conformations between C431 and C1074 predicted from the human P-gp homology model are 36 and 32 Å, respectively. With N611C and T1256C, the predicted distances in the apo and closed conformations are 56 and 39 Å, respectively.

With these cysteine mutations introduced into the NBDs, we first determined the expression of these mutants in insect cells as well as in the BacMam baculovirus-transduced HeLa cells.[12] As seen in Figure 2, the expression and transport function of these mutant P-gps (C431/C1074 and N611C/T1256C) are similar to those of Cys-less WT.

Upon incubation with cross-linkers M14M and M17M with spacer arm lengths of 20 and 25 Å, respectively, disulfide cross-linking between C431 and C1074 was observed in the apo conformation but not in the ADP-V_i trapped conformation (Figure 3). On the basis of the homology model of the human P-gp in the apo conformation (Figure 1), the C431 and C1074 residues are exposed and freely accessible for cross-linking with rigid cross-linkers M14M and M17M with different spacer arm lengths when P-gp is in the apo conformation. Consistent with the homology model, we showed that cross-linking is possible between the two cysteine residues, as evidenced by a cross-linked species as seen in Figure 3. Our data also showed that the NBDs of human P-gp can be separated by distances (20–25 Å) shorter than the reported distances between the NBDs in the X-ray crystal structures of mouse P-gp (36 Å) and the recently reported *C. elegans* P-gp (54 Å). Considering that the distance between the C431 and C1074 residues decreases from 36 to 32 Å when going from the open to closed conformation, the shorter distance of 20–25 Å observed upon cross-linking might be explained by a sliding, lateral movement of the NBDs relative to each other, different from the movement they use to form the closed conformation. This observed movement of the NBDs is consistent with the recently described highly dynamic nature of P-gp in the open conformation.[25]

From this study, it appears that the minimal distance between NBDs appears to be 20–25 Å, as M8M with a spacer linker of 13 Å failed to cross-link C431 and C1074. The NBDs

dx.doi.org/10.1021/bi4007786 | *Biochemistry* 2013, 52, 7327–7338

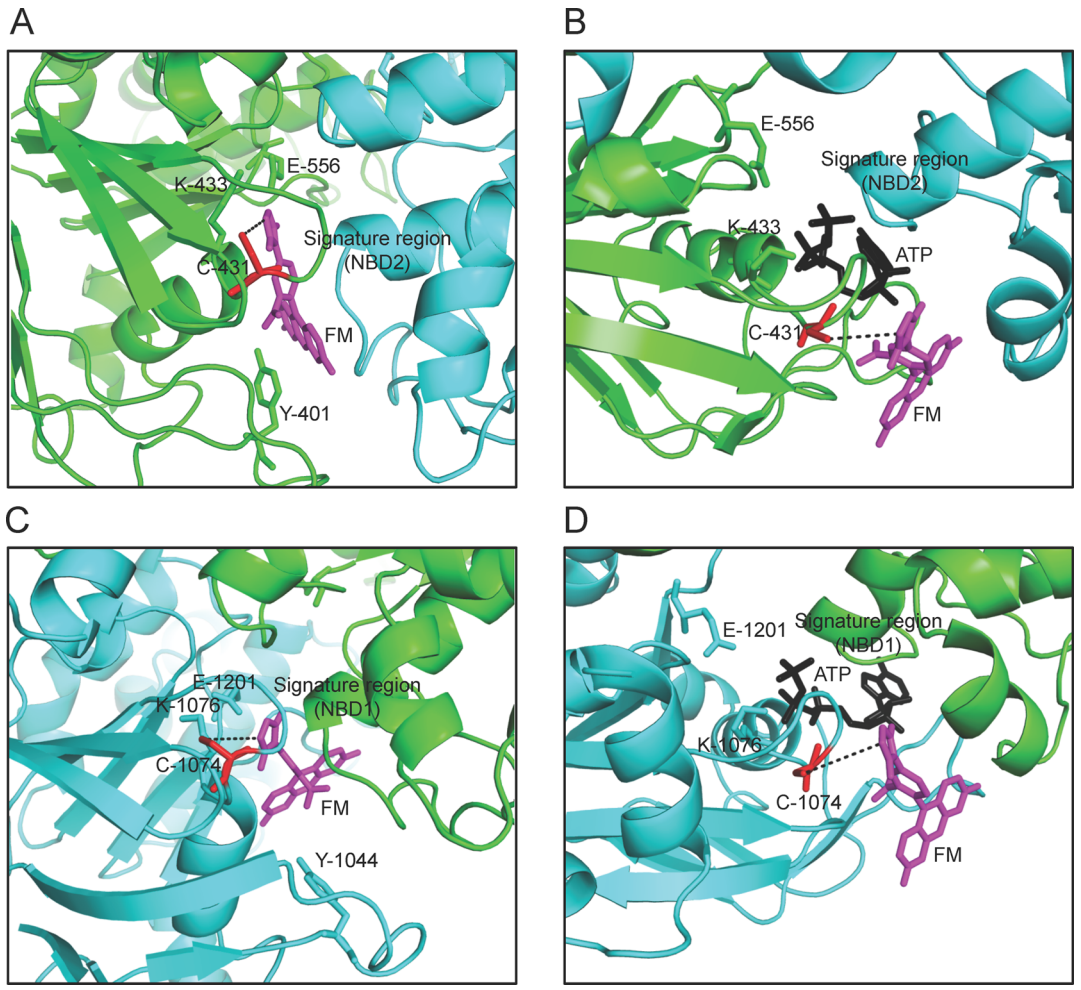

Figure 7. Modeling of orientations of conserved C431 in NBD1 and C1074 in NBD2 in human P-gp. The homology model of NBDs of human P-gp using the HlyB NBD structure was generated as described in Experimental Procedures. (A) Modeling of FM at NBD1 in the absence of ATP. The FM molecule is docked at NBD1 using Vina-Autodock, with the maleimide moiety directed toward C431 for thiol modification. K433 is made flexible for the docking of FM in NBD1. (B) Modeling of FM at NBD1 in the presence of ATP. C431 is oriented outward for chemical reaction with the maleimide moiety of FM. (C) Modeling of FM at NBD2 in the absence of ATP. The FM molecule is docked at NBD2 using Vina-Autodock, with the maleimide moiety directed toward C1074 for thiol modification. (D) Modeling of FM at NBD2 in the presence of ATP. C1074 is oriented outward for chemical reaction with the maleimide moiety of FM. Selected residues are shown as stick models and labeled. The NBD model is shown in two orientations: (A and B) NBD1 to the left and NBD2 to the right and (C and D) NBD1 to the right and NBD2 to the left. The figure is colored as follows: NBD1 in green, NBD2 in cyan, ATP in black, FM in magenta, and C431 and C1074 in red. This figures was created with PyMOL (The PyMOL Molecular Graphics System, Schrodinger, LLC).

might be farther apart (>25 Å), but because of the lack of availability of cross-linkers with arm lengths of >25 Å, we were not able to evaluate this possibility experimentally.

To rule out the possibility that the observed cross-linked P-gp band is due to formation of an intermolecular disulfide between two molecules of cysteine mutant C431/C1074, we conducted disulfide cross-linking with M17M in single C431 and C1074 mutants and in the presence and absence of 5% β-ME (a reducing agent). No cross-linked band was observed with the single-cysteine (C431 and C1074) mutants (Figure S1 of the Supporting Information), and there was no difference seen in the mobility of single-mutant P-gps in the presence or absence of β-ME (data not shown).

On the other hand, in the closed conformation (in the presence of ADP-V_i), there was no cross-linking with M14M or M17M. As there is no X-ray crystal structure of P-gp reported in the presence of bound ATP, we built a homology model of human P-gp in the closed conformation based on the crystal structure of Sav1866 (a bacterial ortholog of human P-gp) and the Hly-B crystal structure. The model clearly shows that there is no space available for the cross-linker to be accommodated at the interface of the NBDs, thus explaining the absence of cross-linking in the ADP-V_i trapped (closed) conformation.

Our results demonstrate that (1) the two native cysteines 431 and 1074 are accessible in both the apo and ADP-V_i trapped conformations to thiol-specific probes such as FM, MTS-verapamil, and/or MTS-rhodamine and (2) there are differences in the degree of accessibility between C431 and C1074, with C1074 being more accessible to FM than C431. This observation is consistent with the report by Loo and Clarke[26] indicating that C1074 is more accessible to NEM (also a thiol-reactive probe) than C431. This difference in accessibility between the two native cysteines in the apo state and in the presence ADP-V_i suggests structural asymmetry in the NBDs, a feature of the P-gp NBDs also observed by Vigano et al.[27]

The greater accessibility associated with C1074 than with C431 is also evidenced by their ATPase activities (Figure 5).

dx.doi.org/10.1021/bi4007786 | *Biochemistry* 2013, 52, 7327−7338

When 5 mM ATP was added prior to treatment with FM, the ATPase activity of C1074 was restored to a lower level of 34%, compared to C431 with recovery of ATPase activity of 62%. With other thiol-reactive probes, such as MTS-verapamil and MTS-rhodamine, a similar conclusion was reached, supporting the greater accessibility of C1074 than of C431. Furthermore, the inhibition of ATPase activity of the NBD cysteine mutants after reaction with probes such as MTS-verapamil (molecular weight of 673.72) and MTS-rhodamine (molecular weight of 695.88) also illustrated that the ATP pockets of both NBDs are accessible to molecules larger than ATP.

In this study, we docked FM in the ATP sites to explain the accessibility of the double-cysteine mutant C431/C1074 to FM in the apo and closed (ADP-V_i trapped) conformations. In the C431/C1074 double-cysteine mutant, there is a similar extent of labeling with FM in both the apo and ADP-V_i trapped closed conformations. A similar extent of FM labeling was observed in both the apo and closed conformations when the ATP pocket was saturated with ATP (in the presence of 20 mM ATP). How is it possible to access the cysteine residues at the Walker A motif when the nucleotide is bound to the NBDs? This accessibility could possibly result from the change in the orientation of the sulfur atoms of C431 and C1074 from inward-facing to outward-facing with respect to the ATP pocket (Figure 7). In the absence of ATP, FM is able to occupy the ATP pocket and the maleimide moiety is directed toward the sulfur atom for covalent labeling of the cysteine. The accessibility of C1074 is slightly higher than that of C431, as reflected by the concentration of FM required to inhibit ATPase activity (IC_{50} values of 0.7 and 1.1 μM, respectively). These results indicate that covalent modification of just one cysteine in the NBD is sufficient to inhibit ATPase activity, an observation consistent with that reported by Urbatsch et al.[28] and Loo et al.[26]

Structural information from the X-ray crystal structures of the maltose importer[29] shows the sulfur atoms of the Walker A cysteines in an inward orientation, facing the ATP pocket. Sav1866[22] has a glycine residue instead of cysteine, and Hyl-B has a serine residue, which is, however, also oriented inward. Our results suggest that the Walker A cysteines can adopt an outward orientation, at least in human P-gp, and do not form strong interactions with the ATP molecule. This interpretation is supported by modeling studies that show an FM molecule can be docked outside the ATP site with the cysteine residues adopting an outward orientation. This is consistent with reports that substitution of these cysteine residues with alanine in Cys-less WT has no effect on ATP binding or hydrolysis at the NDBs or on binding of the substrate at the drug binding pocket in TMDs.[8]

We also investigated the effect of disulfide cross-linking in the presence of drug substrates of P-gp. Disulfide cross-linking of cysteine residues with M17M in the NBDs is still observed with the binding of known P-gp substrates in TMDs (Figure S7 of the Supporting Information), an observation also made by Loo and Clarke.[30] In addition, labeling with FM in the absence or presence of CsA does not change. This indicates that the binding of transport substrates in the TMDs, in the absence of ATP, does not change the accessibility of these cysteines toward covalent modification by thiol-reactive probes.

In summary, the knowledge gained through these studies concerning the accessibility of Walker A cysteines in human P-gp in both the apo and ADP-V_i trapped conformations to thiol-modifying agents is useful, as it can be applied in techniques that map conformational changes of P-gp and improves our understanding of its catalytic cycle.

■ ASSOCIATED CONTENT

Supporting Information

Supplementary table and Figures S1−S7. This material is available free of charge via the Internet at http://pubs.acs.org.

■ AUTHOR INFORMATION

Corresponding Author

*Laboratory of Cell Biology, Center for Cancer Research, National Cancer Institute, National Institutes of Health, Bethesda, MD 20892. E-mail: ambudkar@mail.nih.gov. Phone: (301) 402-4178.

Funding

This research is supported by the Intramural Research Program of the National Institutes of Health, National Cancer Institute, Center for Cancer Research. H.-M.S. is supported in part by a NUS-OPF fellowship from the Department of Pharmacy, Faculty of Science, National University of Singapore.

Notes

The authors declare no competing financial interest.

■ ACKNOWLEDGMENTS

We thank Kenneth Schmidt, Samantha Green, and Adam Gonzalez for technical help and Mr. George Leiman for editorial assistance in the preparation of the manuscript.

■ ABBREVIATIONS

ABC, ATP-binding cassette; P-gp, P-glycoprotein; MDR, multidrug resistance; NBDs, nucleotide-binding domains; TMDs, transmembrane domains; V_i, sodium orthovanadate; FM, fluorescein 5-maleimide; MTS, methanethiosulfonate; M8M, 3,6-dioxaoctane-1,8-diyl bismethanethiosulfonate; M14M, 3,6,9,12-tetraoxatetradecane-1,14-diyl ismethanethiosulfonate; M17M, 3,6,9,12,15-pentaoxaheptadecane-1,17-diyl bismethanethiosulfonate; NEM, *N*-ethylmaleimide; CsA, cyclosporine A; DTT, dithiothreitol.

■ REFERENCES

(1) Dean, M., and Annilo, T. (2005) Evolution of the ATP-binding cassette (ABC) transporter superfamily in vertebrates. *Annu. Rev. Genomics Hum. Genet. 6*, 123−142.

(2) Gottesman, M. M., and Ambudkar, S. V. (2001) Overview: ABC transporters and human disease. *J. Bioenerg. Biomembr. 33*, 453−458.

(3) Aller, S. G., Yu, J., Ward, A., Weng, Y., Chittaboina, S., Zhuo, R., Harrell, P. M., Trinh, Y. T., Zhang, Q., Urbatsch, I. L., and Chang, G. (2009) Structure of P-glycoprotein reveals a molecular basis for poly-specific drug binding. *Science 323*, 1718−1722.

(4) Jin, M. S., Oldham, M. L., Zhang, Q., and Chen, J. (2012) Crystal structure of the multidrug transporter P-glycoprotein from *Caenorhabditis elegans*. *Nature 490*, 566−569.

(5) Sauna, Z. E., Kim, I. W., Nandigama, K., Kopp, S., Chiba, P., and Ambudkar, S. V. (2007) Catalytic cycle of ATP hydrolysis by P-glycoprotein: Evidence for formation of the E·S reaction intermediate with ATP-γ-S, a nonhydrolyzable analogue of ATP. *Biochemistry 46*, 13787−13799.

(6) Loo, T. W., Bartlett, M. C., and Clarke, D. M. (2004) Disulfide cross-linking analysis shows that transmembrane segments 5 and 8 of human P-glycoprotein are close together on the cytoplasmic side of the membrane. *J. Biol. Chem. 279*, 7692−7697.

(7) Loo, T. W., Bartlett, M. C., and Clarke, D. M. (2006) Transmembrane segment 7 of human P-glycoprotein forms part of the drug-binding pocket. *Biochem. J. 399*, 351−359.

(8) Loo, T. W., and Clarke, D. M. (1995) Membrane topology of a cysteine-less mutant of human P-glycoprotein. *J. Biol. Chem. 270*, 843−848.
(9) Sauna, Z. E., Muller, M., Peng, X. H., and Ambudkar, S. V. (2002) Importance of the conserved Walker B glutamate residues, 556 and 1201, for the completion of the catalytic cycle of ATP hydrolysis by human P-glycoprotein (ABCB1). *Biochemistry 41*, 13989−14000.
(10) Ramachandra, M., Ambudkar, S. V., Chen, D., Hrycyna, C. A., Dey, S., Gottesman, M. M., and Pastan, I. (1998) Human P-glycoprotein exhibits reduced affinity for substrates during a catalytic transition state. *Biochemistry 37*, 5010−5019.
(11) Kerr, K. M., Sauna, Z. E., and Ambudkar, S. V. (2001) Correlation between steady-state ATP hydrolysis and vanadate-induced ADP trapping in human P-glycoprotein. Evidence for ADP release as the rate-limiting step in the catalytic cycle and its modulation by substrates. *J. Biol. Chem. 276*, 8657−8664.
(12) Shukla, S., Schwartz, C., Kapoor, K., Kouanda, A., and Ambudkar, S. V. (2012) Use of Baculovirus BacMam Vectors for Expression of ABC Drug Transporters in Mammalian Cells. *Drug Metab. Dispos. 40*, 304−312.
(13) Ambudkar, S. V. (1998) Drug-stimulatable ATPase activity in crude membranes of human MDR1-transfected mammalian cells. *Methods Enzymol. 292*, 504−514.
(14) Altschul, S. F., Madden, T. L., Schaffer, A. A., Zhang, J., Zhang, Z., Miller, W., and Lipman, D. J. (1997) Gapped BLAST and PSI-BLAST: A new generation of protein database search programs. *Nucleic Acids Res. 25*, 3389−3402.
(15) Laskowski, R. A., Macarthur, M. W., Moss, D. S., and Thornton, J. M. (1993) Procheck: A Program to Check the Stereochemical Quality of Protein Structures. *J. Appl. Crystallogr. 26*, 283−291.
(16) Emsley, P., and Cowtan, K. (2004) Coot: Model-building tools for molecular graphics. *Acta Crystallogr. D60*, 2126−2132.
(17) Ohnuma, S., Chufan, E., Nandigama, K., Jenkins, L. M. M., Durell, S. R., Appella, E., Sauna, Z. E., and Ambudkar, S. V. (2011) Inhibition of Multidrug Resistance-Linked P-Glycoprotein (ABCB1) Function by 5′-Fluorosulfonylbenzoyl 5′-Adenosine: Evidence for an ATP Analogue That Interacts with Both Drug-Substrate-and Nucleotide-Binding Sites. *Biochemistry 50*, 3724−3735.
(18) Brooks, B. R., Brooks, C. L., Mackerell, A. D., Nilsson, L., Petrella, R. J., Roux, B., Won, Y., Archontis, G., Bartels, C., Boresch, S., Caflisch, A., Caves, L., Cui, Q., Dinner, A. R., Feig, M., Fischer, S., Gao, J., Hodoscek, M., Im, W., Kuczera, K., Lazaridis, T., Ma, J., Ovchinnikov, V., Paci, E., Pastor, R. W., Post, C. B., Pu, J. Z., Schaefer, M., Tidor, B., Venable, R. M., Woodcock, H. L., Wu, X., Yang, W., York, D. M., and Karplus, M. (2009) CHARMM: The Biomolecular Simulation Program. *J. Comput. Chem. 30*, 1545−1614.
(19) Trott, O., and Olson, A. J. (2010) Software News and Update AutoDock Vina: Improving the Speed and Accuracy of Docking with a New Scoring Function, Efficient Optimization, and Multithreading. *J. Comput. Chem. 31*, 455−461.
(20) Sanner, M. F. (1999) Python: A programming language for software integration and development. *J. Mol. Graphics Modell. 17*, 57−61.
(21) O'Mara, M. L., and Tieleman, D. P. (2007) P-glycoprotein models of the apo and ATP-bound states based on homology with Sav1866 and MalK. *FEBS Lett. 581*, 4217−4222.
(22) Dawson, R. J., and Locher, K. P. (2006) Structure of a bacterial multidrug ABC transporter. *Nature 443*, 180−185.
(23) Schmitt, L., Benabdelhak, H., Blight, M. A., Holland, I. B., and Stubbs, M. T. (2003) Crystal structure of the nucleotide-binding domain of the ABC-transporter haemolysin B: Identification of a variable region within ABC helical domains. *J. Mol. Biol. 330*, 333−342.
(24) Loo, T. W., Bartlett, M. C., and Clarke, D. M. (2003) Simultaneous binding of two different drugs in the binding pocket of the human multidrug resistance P-glycoprotein. *J. Biol. Chem. 278*, 39706−39710.
(25) Wen, P. C., Verhalen, B., Wilkens, S., McHaourab, H. S., and Tajkhorshid, E. (2013) On the Origin of Large Flexibility of P-glycoprotein in the Inward-facing State. *J. Biol. Chem. 288*, 19211−19220.
(26) Loo, T. W., and Clarke, D. M. (1995) Covalent modification of human P-glycoprotein mutants containing a single cysteine in either nucleotide-binding fold abolishes drug-stimulated ATPase activity. *J. Biol. Chem. 270*, 22957−22961.
(27) Vigano, C., Julien, M., Carrier, I., Gros, P., and Ruysschaert, J. M. (2002) Structural and functional asymmetry of the nucleotide-binding domains of P-glycoprotein investigated by attenuated total reflection Fourier transform infrared spectroscopy. *J. Biol. Chem. 277*, 5008−5016.
(28) Urbatsch, I. L., Gimi, K., Wilke-Mounts, S., Lerner-Marmarosh, N., Rousseau, M. E., Gros, P., and Senior, A. E. (2001) Cysteines 431 and 1074 are responsible for inhibitory disulfide cross-linking between the two nucleotide-binding sites in human P-glycoprotein. *J. Biol. Chem. 276*, 26980−26987.
(29) Oldham, M. L., and Chen, J. (2011) Snapshots of the maltose transporter during ATP hydrolysis. *Proc. Natl. Acad. Sci. U.S.A. 108*, 15152−15156.
(30) Loo, T. W., and Clarke, D. M. (2000) Drug-stimulated ATPase activity of human P-glycoprotein is blocked by disulfide cross-linking between the nucleotide-binding sites. *J. Biol. Chem. 275*, 19435−19438.